

**IRON TEREPHTHALATE METAL ORGANIC  
FRAMEWORK DERIVED rGO/Fe<sub>2</sub>O<sub>3</sub>/TiO<sub>2</sub>  
THIN FILM FOR PHOTOCATALYTIC  
DEGRADATION OF METHYLENE  
BLUE DYE IN WATER**



**HASMIRA BINTI RADDE**

**UMS**  
UNIVERSITI MALAYSIA SABAH

**FACULTY OF SCIENCE AND NATURAL  
RESOURCES  
UNIVERSITY MALAYSIA SABAH  
2017**

**IRON TEREPHTHALATE METAL ORGANIC  
FRAMEWORK DERIVED rGO/Fe<sub>2</sub>O<sub>3</sub>/TiO<sub>2</sub>  
THIN FILM FOR PHOTOCATALYTIC  
DEGRADATION OF METHYLENE  
BLUE DYE IN WATER**

**HASMIRA BINTI RADDE**



**A THESIS SUBMITTED IN FULFILLMENT  
WITH THE REQUIREMENT FOR THE DEGREE  
OF MASTER OF SCIENCE**

**FACULTY OF SCIENCE AND NATURAL  
RESOURCES  
UNIVERSITY MALAYSIA SABAH  
2017**

## **DECLARATION**

I hereby declare that the material in this thesis is my own except for quotations, excerpts, equations, summaries and references, which have been duly acknowledged.

18<sup>th</sup> June 2017

.....  
Hasmira binti Radde  
MS1311003T



**UMS**  
UNIVERSITI MALAYSIA SABAH

## CERTIFICATION

NAME : **HASMIRA BINTI RADDE**  
MATRIC NO. : **MS1311003T**  
TITLE : **IRON TEREPHTHALATE METAL ORGANIC FRAMEWORK  
DERIVED rGO/Fe<sub>2</sub>O<sub>3</sub>/TiO<sub>2</sub> THIN FILM FOR  
PHOTOCATALYTIC DEGRADATION OF METHYLENE BLUE  
DYE IN WATER**  
DEGREE : **MASTER OF SCIENCE (INDUSTRIAL CHEMISTRY)**  
VIVA DATE : **28<sup>TH</sup> APRIL 2017**



**CERTIFIED BY;**  
**UMS**  
UNIVERSITI MALAYSIA SABAH  
Signature

---

## ACKNOWLEDGEMENTS

First and foremost, I would like to express my deepest gratitude to Allah for His blessing, Alhamdulillah, I am able to complete this master study.

I would like to acknowledge and thank to my supervisor, Dr Moh Pak Yan, for his continuous support, patience, motivation and dedicated guidance. I really appreciate his leadership in guiding me throughout this study I have grown up as a student with a high degree of competency.

I would like to convey my deepest appreciation and gratitude to University Malaysia Sabah (UMS) and the Faculty Science and Natural Resources (FSSA) for providing me laboratory instruments and apparatus that was needed during my research study. I would like to take this opportunity to thank the industrial chemistry lab assistant, Mr Jerry Alaxender, Mr Racheidy, Mr Taipin, Mr Abdul Rahim and Mr Neldin for their great helps assisting me in handling instruments while doing my lab works.

I would like to thank my green chemistry laboratory colleagues, Nurul Wafa, Sing Yew, Suzanna, Michelle and Veon Fei for their help as well as sharing wonderful ideas and discussions on the projects. My sincere appreciation to my dear family especially my parents, Darwinah and Radde for raising me with love and support me continuously in whatever I do. Special thanks to Herwansyah for his unconditional motivation, constant support and encouragement throughout this master study. Not forgetting my dearest postgraduate mates Nurul Fatihah, Syazreyenna, Noreahan, Nurazilah, Diana, Laurencia and Hanirah, thank you guys for motivating and encouraging me through all the hardness during this study. Last but not least, I also appreciate the financial support from the UMS grant research (ERGS grant: ERGS 0032-STG-01/2-13) and the My Brains Scholarship from the Ministry of Higher Education.

Hasmira Binti Radde  
18<sup>th</sup> June 2017

## ABSTRACT

The major limitations of the photocatalytic activity involving  $\text{TiO}_2$  photocatalyst are difficulty to isolate its powder from treated water, desorption of organic pollutants, high band gap energy and rapid recombination between the charge carriers ( $e^-/h^+$  pairs). This study focuses on the modification of  $\text{TiO}_2$  thin film in order to obtain a better degree of degradation by incorporating small amount of iron terephthalate metal organic framework, MIL-53(Fe) and reduced graphene oxide, rGO to the titania thin film (as rGO/ $\text{Fe}_2\text{O}_3$ / $\text{TiO}_2$  thin film). The rGO/ $\text{Fe}_2\text{O}_3$ / $\text{TiO}_2$  thin films were fabricated via dip coating technique onto a glass substrate. SEM images showed that the coating can be repeated up to 5 cycles and rGO smooth planar sheets were attached to the  $\text{Fe}_2\text{O}_3$ / $\text{TiO}_2$  thin film. EDX analysis showed the presence of small amount of  $\text{Fe}^{3+}$  ions in  $\text{TiO}_2$  thin film. The effect of concentration of MIL-53(Fe), number of dip coating cycle and rGO content were evaluated through the photocatalytic degradation of methylene blue (MB) dye in water under UV-A light for 4 hours. It was found that the highest photocatalytic activity of MB could be obtained using concentration 0.005 wt% of MIL-53(Fe) with 5 dip coating cycles in 0.4 mg/mL of rGO content. This study revealed that the rGO/ $\text{Fe}_2\text{O}_3$ / $\text{TiO}_2$  thin film exhibits a better photocatalytic degradation as it can degrade about 84.0% of 5 ppm MB in water under UV-A irradiation as compared to  $\text{TiO}_2$  thin film alone which can only degrade 68.5% MB. The total enhancement of the rGO/ $\text{Fe}_2\text{O}_3$ / $\text{TiO}_2$  thin film was about 16%. The study on photocatalytic degradation of 5 ppm MB under visible light shows that rGO/ $\text{Fe}_2\text{O}_3$ / $\text{TiO}_2$  able to degrade 46.7% of MB whereas  $\text{TiO}_2$  thin film alone was only 36.2%. A slight improvement which was about 10% of MB removal was obtained under visible light which means the incorporation of rGO has slightly reduced the band gap of  $\text{TiO}_2$  thin film. A better degree of degradation can also attributed to the better adsorption property of rGO/ $\text{Fe}_2\text{O}_3$ / $\text{TiO}_2$  in comparison to that of  $\text{TiO}_2$  and  $\text{Fe}_2\text{O}_3$ / $\text{TiO}_2$  thin film. In dark condition, rGO/ $\text{Fe}_2\text{O}_3$ / $\text{TiO}_2$  thin film and  $\text{TiO}_2$  thin film alone can degrade 29.5% and 24.5%, respectively. About 5% enhancement was obtained in dark after incorporation of rGO and MIL-53(Fe). The rGO/ $\text{Fe}_2\text{O}_3$ / $\text{TiO}_2$  thin film posses a good stability and can be reuse up to 3 cycles without activation. The performance of the rGO/ $\text{Fe}_2\text{O}_3$ / $\text{TiO}_2$  thin film follows the pseudo-first-order reaction kinetic with the rate constant  $0.007 \text{ min}^{-1}$  which is almost double as compared to  $\text{TiO}_2$  thin film alone. The rGO/ $\text{Fe}_2\text{O}_3$ / $\text{TiO}_2$  thin film has high potential to be applied in wastewater treatment field and also as a tinting material for households and industries to provide self cleaning property.

## **ABSTRAK**

### **SAPUT TIPIS $rGO/Fe_2O_3/TiO_2$ YANG DIPEROLEH DARIPADA KERANGKA BESI ORGANIK 'IRON TEREPHTHALATE' UNTUK DEGRADASI FOTOPEMANGKINAN KEATAS PEWARNA METILIN BIRU (MB) DI DALAM AIR**

Permasalahan utama didalam aktiviti pemangkinanfoto melibatkan pemangkinfoto  $TiO_2$  adalah kesukaran untuk mengasingkan serbuknya dari air yang telah dirawat, penyahserapan bahan pencemar organik, ruang jalur yang tinggi dan pergabungan yang pantas diantara pembawa cas (pasangan  $e^-/h^+$ ). Kajian ini memfokuskan pengubahsuaian keatas saput tipis  $TiO_2$  untuk mendapatkan degradasi yang lebih baik dengan menggabungkan kerangka besi organik 'iron terephthalate', MIL-53(Fe) dan 'reduced graphene oxide', rGO kedalam saput tipis titania (sebagai  $rGO/Fe_2O_3/TiO_2$ ). Saput tipis  $rGO/Fe_2O_3/TiO_2$  telah difabrikasikan menggunakan teknik rendam celup keatas penyokong kaca. Imej SEM menunjukkan lapisan saput nipis boleh diulang sehingga 5 kitaran dan ke atas serta kepingan rata satah rGO berhubung dipermukaan saput tipis  $Fe_2O_3/TiO_2$ . Analisis EDX menunjukkan kehadiran bilangan yang terlalu sedikit ion  $Fe^{3+}$  didalam saput tipis  $TiO_2$ . Kesan terhadap kepekatan MIL-53(Fe), bilangan kitaran lapisan dan kandungan rGO ditentukan melalui degradasi pemangkinanfoto keatas pewarna Metilin Biru (MB) didalam air dibawah sinaran cahaya UV-A selama 4 jam. Kajian mendapati nilai tertinggi aktiviti fotopemangkinan ke atas MB boleh diperolehi dengan menggunakan 0.005 wt% MIL-53(Fe) dengan 5 lapisan dan kandungan rGO sebanyak 0.4 mg/mL. Kajian ini membuktikan saput tipis  $rGO/Fe_2O_3/TiO_2$  mempunyai kelebihan yang lebih baik didalam degradasi pemangkinanfoto dimana ianya mampu mendegradasikan sebanyak 84.0% 5 ppm MB didalam air dibawah sinaran UV-A berbanding dengan saput tipis  $TiO_2$  sendiri yang hanya mampu mendegradasi sebanyak 68.5% MB sahaja. Jumlah peningkatan bagi saput tipis  $rGO/Fe_2O_3/TiO_2$  adalah sebanyak 16%. Kajian degradasi pemangkinanfoto ke atas 5ppm MB dibawah sinaran cahaya nampak menunjukkan saput tipis  $rGO/Fe_2O_3/TiO_2$  berupaya mendegradasikan sebanyak 46.7% pewarna MB manakala saput tipis  $TiO_2$  sendiri hanya 36.2%. Sebanyak 10% peningkatan didalam penyingkiran MB telah diperolehi dibawah cahaya nampak dimana penggabungan rGO telah mengurangkan ruang jalur saput tipis  $TiO_2$ . Tahap degradasi yang lebih baik juga adalah disebabkan ciri-ciri penjerapan saput tipis  $rGO/Fe_2O_3/TiO_2$  berbanding dengan saput tipis  $TiO_2$  dan  $Fe_2O_3/TiO_2$ . Dalam keadaan gelap pula, saput tipis  $rGO/Fe_2O_3/TiO_2$  dan  $TiO_2$  masing-masing boleh mendegradasi sebanyak 29.5% dan 24.5%. Sebanyak 5% peningkatan yang telah diperolehi di dalam keadaan gelap selepas penggabungan rGO dan MIL-53(Fe). Saput tipis  $rGO/Fe_2O_3/TiO_2$  mempunyai kestabilan yang baik dan boleh digunapakai sehingga 3 kitaran tanpa perlu diaktifkan. Prestasi saput tipis  $rGO/Fe_2O_3/TiO_2$

*mematuhi 'pseudo-first-order reaction kinetic' dengan kadar tetap  $0.007\text{min}^{-1}$  yang mana menghampiri dua kali ganda jika dibandingkan dengan saput tipis  $\text{TiO}_2$  sendiri. Saput tipis  $\text{rGO/Fe}_2\text{O}_3/\text{TiO}_2$  mempunyai potensi yang baik untuk digunakan didalam bidang rawatan air sisa dan juga sebagai bahan lapisan untuk peralatan rumah dan industri yang boleh memberikan kesan pembersihan sendiri.*



UMS  
UNIVERSITI MALAYSIA SABAH

# TABLE OF CONTENTS

	Page
<b>TITLE</b>	i
<b>DECLARATION</b>	ii
<b>CERTIFICATION</b>	iii
<b>ACKNOWLEDGEMENTS</b>	iv
<b>ABSTRACT</b>	v
<b>ABSTRAK</b>	vi
<b>TABLE OF CONTENTS</b>	viii
<b>LIST OF TABLES</b>	xii
<b>LIST OF FIGURE</b>	xiii
<b>LIST OF ABBREVIATIONS AND SYMBOLS</b>	xvii
<b>CHAPTER 1: INTRODUCTION</b>	1
1.1 Introduction	1
1.2 Drawbacks of TiO <sub>2</sub> Photocatalyst	4
1.3 Objectives	4
1.4 Scopes of Study	4
<b>CHAPTER 2: LITERATURE REVIEW</b>	6
2.1 Dyes and Treatment of Dye Pollutants	6
2.1.1 Conventional Treatment of Dye	8
2.1.2 Current Treatment of Dye	10
2.2 Advanced Oxidation Process (AOP)	11
2.2.1 Types of AOP	11
2.2.2 Photodegradation of Organic Pollutant by TiO <sub>2</sub> /UV	12
2.3 TiO <sub>2</sub> Photocatalyst	15
2.3.1 TiO <sub>2</sub> Powder	19
2.3.2 TiO <sub>2</sub> Thin Film	20
2.3.3 Dopped TiO <sub>2</sub> Thin Film	21
2.4 Hybrid Porous Solid	22

2.4.1	Metal Organic Frameworks (MOFs)	23
2.4.2	Synthesis of MOFs	25
2.4.3	MOFs as Catalyst Support	29
2.4.4	MIL-53(Fe)	32
2.5	Graphene	35
2.5.1	Synthesis of Graphene	37
2.5.2	Chemically Derived Graphene: GO & rGO	43
2.6	Past Research Related To Graphene-Assisted TiO <sub>2</sub> and MOF-Assisted TiO <sub>2</sub>	49
<b>CHAPTER 3: METHODOLOGY</b>		<b>55</b>
3.1	Chemical	55
3.2	Fabrication of Fe <sub>2</sub> O <sub>3</sub> /TiO <sub>2</sub> Thin Film	55
3.2.1	Synthesis of Iron Terephthalate Metal Organic Framework, MIL-53(Fe)	55
3.2.2	Preparation of TiO <sub>2</sub> Sol Gel	56
3.2.3	Preparation of MIL-53(Fe)/TiO <sub>2</sub> Sol Gel	56
3.2.4	Preparation of TiO <sub>2</sub> thin film and Fe <sub>2</sub> O <sub>3</sub> /TiO <sub>2</sub> Thin Film	57
3.3	Fabrication of rGO/Fe <sub>2</sub> O <sub>3</sub> /TiO <sub>2</sub> Thin Film	58
3.3.1	Synthesis of Graphene Oxide (GO)	58
3.3.2	Preparation of GO Suspension	59
3.3.3	Fabrication and Reduction of GO/ Fe <sub>2</sub> O <sub>3</sub> /TiO <sub>2</sub> Thin Film	59
3.4	Characterization of MIL-53(Fe) Powder, GO, TiO <sub>2</sub> Thin Film, Fe <sub>2</sub> O <sub>3</sub> /TiO <sub>2</sub> Thin Film and rGO/Fe <sub>2</sub> O <sub>3</sub> /TiO <sub>2</sub> Thin Film	60
3.4.1	X-Ray Diffraction (XRD)	60
3.4.2	Thermal Gravimetric Analysis (TGA)	61
3.4.3	Fourier Transform Infrared (FTIR)	62
3.4.4	Scanning Electron Microscope – Energy Dispersive X-Ray Spectroscopy (SEM-EDX)	62
3.4.5	Ultraviolet-Visible Spectroscopy (UV-Vis)	64
3.5	Photocatalytic Activity of rGO/Fe <sub>2</sub> O <sub>3</sub> /TiO <sub>2</sub> Thin Film	65
3.5.1	Preparation of Methylene Blue (MB) Solution	65
3.5.2	Set Up of Batch Photoreactor	65

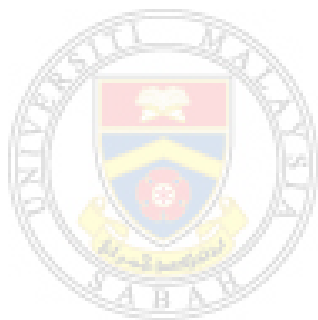
3.5.3	Photocatalytic Degradation of Methylene Blue Solution	66
3.5.4	Reusability test of rGO/Fe <sub>2</sub> O <sub>3</sub> /TiO <sub>2</sub> Thin Film	67
3.5.5	Kinetics of MB Degradation	68
<b>CHAPTER 4: SYNTHESIS AND CHARACTERIZATION OF rGO/Fe<sub>2</sub>O<sub>3</sub>/TiO<sub>2</sub> THIN FILM</b>		<b>70</b>
4.1	MIL-53(Fe) and Graphene Oxide (GO)	70
4.1.1	MIL-53(Fe)	70
4.1.2	Graphene Oxide (GO)	72
4.2	Fabrication of rGO/Fe <sub>2</sub> O <sub>3</sub> /TiO <sub>2</sub> Thin Film	75
4.2.1	XRD Diffractogram of TiO <sub>2</sub> and Fe <sub>2</sub> O <sub>3</sub> /TiO <sub>2</sub> Thin Films	76
4.2.2	Surface Morphology of TiO <sub>2</sub> , Fe <sub>2</sub> O <sub>3</sub> /TiO <sub>2</sub> and rGO/Fe <sub>2</sub> O <sub>3</sub> /TiO <sub>2</sub> Thin Films	77
4.2.3	EDX Analysis of TiO <sub>2</sub> , Fe <sub>2</sub> O <sub>3</sub> /TiO <sub>2</sub> and rGO/Fe <sub>2</sub> O <sub>3</sub> /TiO <sub>2</sub> Thin Films	81
4.2.4	Optical Band Gap Energy of TiO <sub>2</sub> and rGO/Fe <sub>2</sub> O <sub>3</sub> /TiO <sub>2</sub> Thin Films	84
<b>CHAPTER 5: PHOTOCATALYTIC ACTIVITY OF rGO/Fe<sub>2</sub>O<sub>3</sub>/TiO<sub>2</sub> THIN FILM</b>		<b>86</b>
5.1	Stability of MB in Water	86
5.2	Effect of Amount of MIL-53(Fe)	87
5.3	Effect of Dip Coating Cycles	89
5.4	Effect of The Amount of rGO	91
5.5	Effect of The Source of Irradiation	93
5.6	Reusability Test of rGO/Fe <sub>2</sub> O <sub>3</sub> /TiO <sub>2</sub> Thin Film	96
5.7	Kinetics Study of MB Degradation	99
5.8	Mechanism of Photocatalytic Degradation of MB by rGO/Fe <sub>2</sub> O <sub>3</sub> /TiO <sub>2</sub> and TiO <sub>2</sub> Thin Films	102
<b>CHAPTER 6: CONCLUSION &amp; FUTURE RECOMMENDATIONS</b>		<b>105</b>
6.1	Conclusion	105
6.2	Future Recommendation	107

**REFERENCES**

108

**APPENDICES**

121



**UMS**  
UNIVERSITI MALAYSIA SABAH

## LIST OF TABLES

	Page
Table 2.1: Names of chromophores and auxochrome group of dyes	6
Table 2.2: Wavelength of light absorption versus colour in organic dyes	7
Table 2.3: Possible treatments for cotton textile waste and their advantages and disadvantages	9
Table 2.4: Comparison of various electrochemical potential	11
Table 2.5: Basic physical properties of TiO <sub>2</sub>	18
Table 2.6: Criteria of a good support	20
Table 2.7: Summary table synthesis of graphene	42
Table 2.8: Summary of the graphene (its derivatives) assisted TiO <sub>2</sub> composite and its applications	52
Table 2.9: Summary of the MOFs assisted TiO <sub>2</sub> composite and its applications	54
Table 3.1: Concentration of MIL-53(Fe)/TiO <sub>2</sub> Sol Gel	57
Table 3.2: Amount of GO used	59
Table 3.3: Photocatalysis experiment of TiO <sub>2</sub> thin film, Fe <sub>2</sub> O <sub>3</sub> /TiO <sub>2</sub> thin film and rGO/Fe <sub>2</sub> O <sub>3</sub> /TiO <sub>2</sub> thin film with different sample	67
Table 5.1: Summary effect of MIL-53(Fe) concentration in TiO <sub>2</sub> thin films	88
Table 5.2: Summary of effect of number dipping cycle towards TiO <sub>2</sub> thin film and Fe <sub>2</sub> O <sub>3</sub> /TiO <sub>2</sub>	90
Table 5.3: Summary of effect of rGO amount in Fe <sub>2</sub> O <sub>3</sub> /TiO <sub>2</sub> Thin Film	93
Table 5.4: Summary effect of source irradiation towards TiO <sub>2</sub> and rGO/Fe <sub>2</sub> O <sub>3</sub> /TiO <sub>2</sub> thin film	96
Table 5.5: Summary of reusability of TiO <sub>2</sub> thin film and rGO/Fe <sub>2</sub> O <sub>3</sub> /TiO <sub>2</sub> thin film.	99
Table 5.6: Correlation coefficient and rate constant values of pseudo- first and pseudo-second order kinetic models.	101

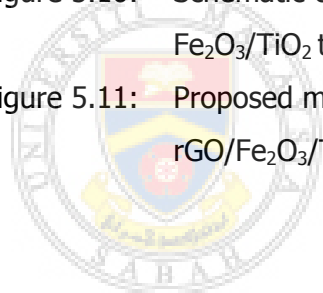
## LIST OF FIGURES

	Page
Figure 1.1: Schematic diagram of semiconductor excitation by band gap illumination leading to the creation of "electrons" in the conduction band and "holes" in the valence band	2
Figure 2.1: Paper published on dye removal according to the process employed	10
Figure 2.2: Various technologies for waste water involving AOPs	12
Figure 2.3: Modified schematic of TiO <sub>2</sub> photocatalytic mechanism	13
Figure 2.4: Application of Titanium Dioxide (TiO <sub>2</sub> )	15
Figure 2.5: Schematic unit cell of four TiO <sub>2</sub> polymorphs. (a) Rutile, (b) Anatase, (c) Brookite, (d) TiO <sub>2</sub> (B)	17
Figure 2.6: Structure of TiO <sub>2</sub> (B)	19
Figure 2.7: A schematic representation of bulk modification by cation-doping	22
Figure 2.8: Schematic representation of the construction of metal organic framework	23
Figure 2.9: Molecular structures of organic linkers used for the synthesis of MOF material	24
Figure 2.10: Different crystal structures of metal organics framework materials	25
Figure 2.11: Conventional solvothermal synthesis of MOF structure	26
Figure 2.12: Mechanochemical synthesis of MOF structure	27
Figure 2.13: Sonochemical synthesis of MOFs structure	28
Figure 2.14: Schematic diagram of the synthesis of microporous brookite from a MOFs template	30
Figure 2.15: Schematic illustration for the synthetic approaches used in for various TiO <sub>2</sub> -based hollow shell photocatalyst. TiO <sub>2</sub> shell, Cu/TiO <sub>2</sub> -AA and Cu/TiO <sub>2</sub> -500°C	31
Figure 2.16: View of the structure of MIL-53(M)	32
Figure 2.17: The breathing behavior of MIL-53 using heat as the external stimulus	33

Figure 2.18:	The chemical structure of MIL-53(Fe)	34
Figure 2.19:	A single graphite sheet consisting of a honeycomb lattice structure of $sp^2$ bonded carbon atoms	35
Figure 2.20:	Scheme showing graphene can be wrapped to a 0D fullerenes, wrapped to form 1D carbon nanotubes (CNTs), or stacked to form 3D graphite	36
Figure 2.21:	The single layer of graphene as first observed by Geim and Novoselov at the University of Manchester	38
Figure 2.22:	Mechanical exfoliation of graphene using scotch tape from HOPG	38
Figure 2.23:	Synthesis of graphene based on Hummer's method using ultrasonication	40
Figure 2.24:	Structure of GO	43
Figure 2.25:	Preparation of graphene by chemical reduction of graphene oxide synthesized by Hummers method	45
Figure 2.26:	Typical optical images of GO solution and rGO solution	46
Figure 2.27:	The idealized and simplified pathway for the reduction of GO by hydrazine hydrate	47
Figure 2.28:	GO-TiO <sub>2</sub> thin film & rGO-TiO <sub>2</sub> thin film on quartz substrate after UV irradiation for 25 minute	48
Figure 2.29:	Schematic illustration of the charge carrier transfer for graphene-semiconductor photocatalyst	50
Figure 3.1:	TiO <sub>2</sub> Sol Gel Precursor	56
Figure 3.2:	Generalized flowchart of MIL-53(Fe)/TiO <sub>2</sub> sol gel preparation	57
Figure 3.3:	Schematic diagram of lab scale dip coating machine	58
Figure 3.4:	Pictorial steps for fabrication of rGO/Fe <sub>2</sub> O <sub>3</sub> /TiO <sub>2</sub> thin film	60
Figure 3.5:	X-Ray Diffractometer (Philips X'Pert Pro IMS)	61
Figure 3.6:	Thermogravimetric analyzer (TGA 6)	61
Figure 3.7:	Fourier transform infrared spectrum 100 (Perkin Elmer)	62
Figure 3.8:	Sputter Coater	63
Figure 3.9:	Scanning electron microscope-energy dispersive X-Ray spectroscopy (SEM-EDX)	63

Figure 3.10:	UV-Vis Spectroscopy (Cary 60; Agilent Technologies)	64
Figure 3.11:	Series of dilution MB dye solution	65
Figure 3.12:	Experimental set up of for photocatalytic degradation of rGO/Fe <sub>2</sub> O <sub>3</sub> /TiO <sub>2</sub> thin film	66
Figure 4.1:	Synthesized MIL-53(Fe) powder and XRD pattern of MIL-53(Fe) crystal	70
Figure 4.2:	TGA analysis of synthesized MIL-53(Fe)	71
Figure 4.3:	GO dispersion in water	72
Figure 4.4:	UV-Vis Spectrum of a 0.01 mg/mL GO aqueous dispersion	73
Figure 4.5:	GO after freeze-dried	73
Figure 4.6:	XRD Pattern of synthesized GO	74
Figure 4.7:	FTIR spectrum of synthesized GO	74
Figure 4.8:	Pictorial of clean glass slide, TiO <sub>2</sub> , Fe <sub>2</sub> O <sub>3</sub> /TiO <sub>2</sub> & rGO/Fe <sub>2</sub> O <sub>3</sub> /TiO <sub>2</sub> thin films	75
Figure 4.9:	XRD pattern of TiO <sub>2</sub> and Fe <sub>2</sub> O <sub>3</sub> /TiO <sub>2</sub> thin films	76
Figure 4.10:	SEM images of (a) five layers TiO <sub>2</sub> thin film deposited on glass & (b) six layers TiO <sub>2</sub> thin film deposited on glass	78
Figure 4.11:	SEM images of five layer Fe <sub>2</sub> O <sub>3</sub> /TiO <sub>2</sub> thin film deposited on glass	79
Figure 4.12:	SEM images of five layer rGO/Fe <sub>2</sub> O <sub>3</sub> /TiO <sub>2</sub> thin film deposited on glass	80
Figure 4.13:	Cross-sectional SEM image of TiO <sub>2</sub> thin film, Fe <sub>2</sub> O <sub>3</sub> /TiO <sub>2</sub> thin film & rGO/Fe <sub>2</sub> O <sub>3</sub> /TiO <sub>2</sub> thin film	81
Figure 4.14:	EDX spectrum of TiO <sub>2</sub> thin film	82
Figure 4.15:	EDX spectrum of Fe <sub>2</sub> O <sub>3</sub> /TiO <sub>2</sub> thin film	83
Figure 4.16:	EDX spectrum of rGO/Fe <sub>2</sub> O <sub>3</sub> /TiO <sub>2</sub> thin film	84
Figure 4.17:	Optical band gap energy of TiO <sub>2</sub> and rGO/Fe <sub>2</sub> O <sub>3</sub> /TiO <sub>2</sub> thin films	85
Figure 5.1:	Degradation of MB	86
Figure 5.2:	Effect of MIL-53(Fe) concentration towards the photocatalytic activity of Fe <sub>2</sub> O <sub>3</sub> /TiO <sub>2</sub> thin film for the degradation of 5 ppm MB in water under UV-A irradiation	87
Figure 5.3:	Effect of dip coating cycle of TiO <sub>2</sub> thin film and Fe <sub>2</sub> O <sub>3</sub> /TiO <sub>2</sub> thin film towards photocatalytic degradation of 5 ppm MB dye in water under UV-A irradiation	89

Figure 5.4:	Effect of the amount of rGO in Fe <sub>2</sub> O <sub>3</sub> /TiO <sub>2</sub> thin film towards photocatalytic degradation of 5 ppm MB dye in water under UV-A irradiation	91
Figure 5.5:	Effect of the source of irradiation of TiO <sub>2</sub> thin film and rGO/Fe <sub>2</sub> O <sub>3</sub> /TiO <sub>2</sub> thin film towards the photocatalytic of 5 ppm MB dye in water under UV-A irradiation	95
Figure 5.6:	Reusability of TiO <sub>2</sub> Thin film and rGO/Fe <sub>2</sub> O <sub>3</sub> /TiO <sub>2</sub> thin film towards photocatalytic degradation of MB dye in water	97
Figure 5.7:	TiO <sub>2</sub> and rGO/Fe <sub>2</sub> O <sub>3</sub> /TiO <sub>2</sub> thin films after 5 cycles of photocatalytic degradation of 3 ppm MB in water	98
Figure 5.8:	Pseudo-first-order-kinetics model of photocatalytic degradation of MB dye in water	99
Figure 5.9:	Pseudo-second-order-kinetics model of photocatalytic degradation of MB dye in water	100
Figure 5.10:	Schematic of photocatalytic degradation mechanisms of Fe <sub>2</sub> O <sub>3</sub> /TiO <sub>2</sub> thin film	102
Figure 5.11:	Proposed mechanism for the photocatalytic activity of rGO/Fe <sub>2</sub> O <sub>3</sub> /TiO <sub>2</sub> thin film	104



## LIST OF ABBREVIATIONS AND SYMBOLS

<b>Abs</b>	- Absorbance
<b>AOPs</b>	- Advanced Oxidation Processes
<b>CB</b>	- Conduction band
<b>Cu<sub>3</sub>(BTC)<sub>2</sub></b>	- Copper (II) benzene-1,3,5-tricarboxylate
<b>CVD</b>	- Chemical vapour deposition
<b>EDX</b>	- Energy Dispersive X-Ray
<b>E<sub>bg</sub></b>	- Band Gap Energy
<b>Fe<sub>2</sub>O<sub>3</sub>/TiO<sub>2</sub></b>	- Ferric Oxide/Titanium Dioxide
<b>FTIR</b>	- Fourier Transform Infrared
<b>GO</b>	- Graphene Oxide
<b>GO/ Fe<sub>2</sub>O<sub>3</sub>/TiO<sub>2</sub></b>	- Graphene Oxide/Ferric Oxide/Titanium Dioxide
<b>hν</b>	- UV light
<b>HKUST-1</b>	- Hong Kong University of Science and Technology 1
<b>HOPG</b>	- Highly Ordered Pyrolytic Graphite
<b>IUPAC</b>	- International Union of Pure and Applied Chemistry
<b>MB</b>	- Methylene Blue
<b>MIL</b>	- Material Institute Lavoisier
<b>MOFs</b>	- Metal organic frameworks
<b>MOF@TiO<sub>2</sub></b>	- Metal organic framework derived titanium dioxide
<b>PAHs</b>	- Polycyclic aromatic hydrocarbons
<b>PCP</b>	- Porous coordination polymers
<b>rGO</b>	- Reduced graphene oxide
<b>rGO/Fe<sub>2</sub>O<sub>3</sub>/TiO<sub>2</sub></b>	- Reduced graphene oxide/Ferric Oxide/Titanium Dioxide
<b>SEM</b>	- Scanning electron microscope
<b>TEM</b>	- Transmission Electron Microscope
<b>TMBDC</b>	- Tetramethylbenzene-1,4-dicarboxylate
<b>UHV</b>	- Ultrahigh vacuum
<b>UV-A</b>	- Ultraviolet A
<b>UV-Vis</b>	- Ultraviolet Visible
<b>VB</b>	- Valence band

# CHAPTER 1

## INTRODUCTION

### 1.1 Introduction

Over the past few decades, advanced oxidation processes (AOPs) has appear to be an alternative to conventional methods used for decolourization of wastewater effluent containing toxic dyes compound (Sharma et al., 2011). Unlike conventional methods which generates new secondary waste and need a high cost of post treatment, AOPs promises a destructive method which destroy the contaminant directly in water through the chemical transformation (Fernández et al.,2010). The key features of AOPs which constitute the generation of hydroxyl radical (OH•) act as strong oxidant to destroy and mineralized contaminant into water (H<sub>2</sub>O), carbon dioxide (CO<sub>2</sub>) and mineral salt (Pelaez *et al.*,2012 ; Sharma *et al.*, 2011). Generally, AOPs can be divided into two types: non irradiation processes and irradiation processes (Sharma *et al.*, 2011).

Photocatalytic degradation based on TiO<sub>2</sub> photocatalyst is an example of AOPs which classified into irradiation process AOPs (Sharma *et al.*, 2011). Among other semiconductors, TiO<sub>2</sub> has been the most commonly studied photocatalyst for the purpose of environmental remediation. This is not only due to its ability to degrade organic pollutants and achieve complete mineralization of the organic contaminants under ultraviolet exposure, but also because TiO<sub>2</sub> has high degradation efficiency to decompose almost any organic contaminant which making it an excellent and effective photocatalyst for the photocatalytic degradation of various organic contaminants (Zhang *et al.*, 2011).

TiO<sub>2</sub> photocatalyst is also largely available, relatively inexpensive and non-toxic. Besides that, it also provides a rapid, environmental friendly, high stability, and an efficient method in the wastewater treatment (Pichat, 2010). Basically, the TiO<sub>2</sub> based photocatalysis is initiated through the photoactivation of TiO<sub>2</sub>. When

exposed with UV light ( $\lambda < 390$  nm), electron at valence band (VB) will excite to conduction band (CB), generating a hole at valence band and forming electron-hole pairs ( $e^-/h^+$ ) as shown in Figure 1.1 These electron-hole pairs induced a series of reaction which lead to the photocatalytic degradation of organic pollutants.

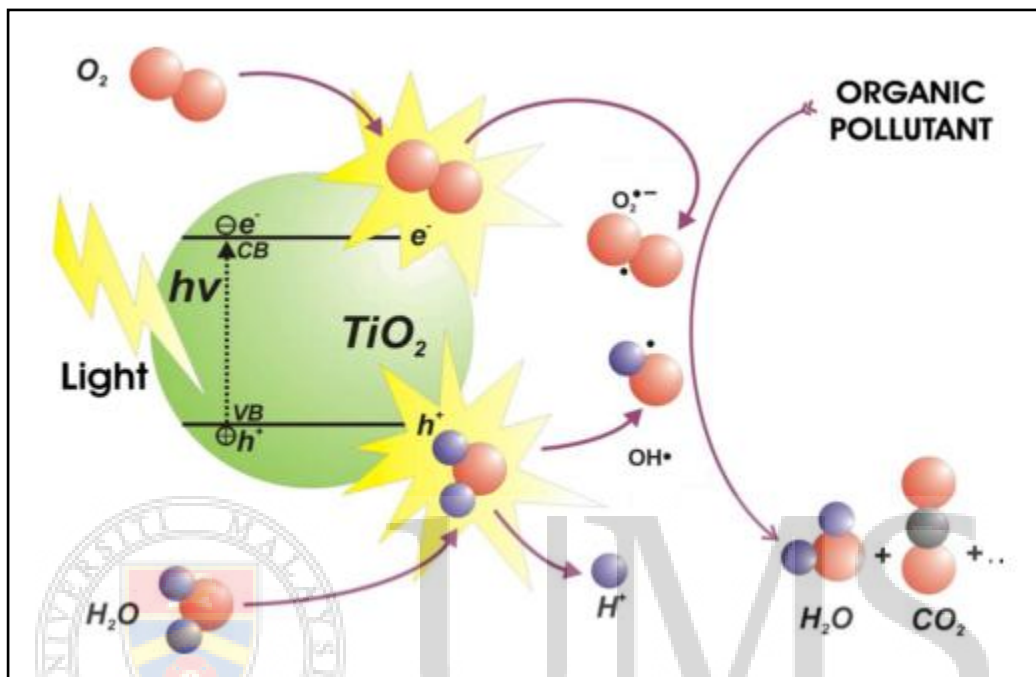


**Figure 1.1 : Schematic diagram of semiconductor excitation by band gap illumination leading to the creation of "electrons" in the conduction band and "holes" in the valence band.**

Source : Ibhaddon & Fitzpatrick (2013)

However, there are a few problems that have arisen which inhibit the full potential of the photocatalytic activity of TiO<sub>2</sub> photocatalyst and thus limiting the application of the photocatalysis process. To date, much effort has been devoted to the modification of the TiO<sub>2</sub> materials in order to enhance their photocatalytic degradation activities (Park *et al.*, 2013). One of the important approaches was by doping or combining various metal, non-metal ions and noble metal to the crystalline TiO<sub>2</sub>. This method commonly used to increase the electron transfer rate at the interface and shift the light absorption towards the visible light region (Mital & Manoj, 2011). Unfortunately, the photocatalytic activity of the synthesized combined material strongly depends on the dopant ion species, concentration of

the dopant and the preparation technique (Li *et al.*, 2012). Moreover, utilization of noble metal (Pt, Pd and Au) in this modification usually involved an expensive cost and not suitable to be applied in massive scale applications. Thus, it is important to replace the noble metal ions with other inexpensive co-catalyst for the development of highly efficient cost effective photocatalyst (Anandan *et al.*, 2013). Apart from that, another modification of TiO<sub>2</sub> which involving immobilization where TiO<sub>2</sub> powder bounded on solid supports or thin film forms can eliminate the high cost of separation process between the TiO<sub>2</sub> powder and the treated water (Pichat, 2013).

MOFs are a new class of advanced porous materials which are composed of metal ions or metal ions clusters (secondary building units) as nodes and organic ligands as linkers (Zhang & Chen, 2013; MacGillivray, 2010). It is expected that incorporating MIL-53(Fe) (a type of MOFs) in TiO<sub>2</sub> photocatalyst would make the metal clusters that interconnected with the MOFs ligands to act as precursor for Fe doped TiO<sub>2</sub> after the thermal treatment. Another new exciting material, graphene and its derivatives, have also been reported as an excellent support for TiO<sub>2</sub> to enhance the photocatalytic activity by facilitate the charge separation, enhanced the adsorption capacity, as well as reducing the band gap of TiO<sub>2</sub> (Ismail *et al.*, 2013). Graphene with a lower Fermi level usually served as 2D electron conductive platform that can accept and transfer electron generated from the band gap photoexcitation of semiconductors, thereby accelerate the separation and transfer of charge carriers to participate in the photoredox process (Zhang *et al.*, 2015).

This study focuses on modification of immobilized TiO<sub>2</sub> thin film by incorporating small amount of MIL-53(Fe) and rGO as co-catalysts. It was expected that the Fe<sub>2</sub>O<sub>3</sub> derived from MIL-53(Fe) could reduce the recombination of electrons-holes pairs and allow the absorption of visible light. To enhance the photocatalytic activity more, outer layer of thin film will be added with two dimensional planar structure rGO layer which served as 2D electron conductive platform. The efficiency of the material was evaluated through the photocatalytic degradation towards methylene blue (MB) under UV-A irradiation.

## 1.2 Drawbacks of TiO<sub>2</sub> Photocatalyst

The main problems that restrict the photoactivity of TiO<sub>2</sub> materials are the rapid recombination of the photogenerated electron/holes pairs. When recombination occurs, the excited electron will return back to valence band without reacting with the adsorbed species (Mital & Manoj, 2011). Therefore, the efficient consumption of electrons is essential to promote photocatalytic oxidation (Kaneko & Okura, 2002). Another problem encountered by TiO<sub>2</sub> materials are the low mass transport rates between the active centres of TiO<sub>2</sub> photocatalyst and the organic pollutants and also the associated issues of nanoparticle separation (Wang & Curaso, 2011). Besides, narrow light response range also has limits the photoactivity of TiO<sub>2</sub> photocatalyst and hinder its practical applications (Park *et al.*, 2013). High band gap of TiO<sub>2</sub> (3.21 eV for anatase) semiconductor required only high energy of UV light (achievable from only 5% of sunlight) to be photoexcited (Mahmood *et al.*, 2014; Tan *et al.*, 2012; Wang & Curaso, 2011). Thus, bare TiO<sub>2</sub> has limited photocatalytic activity in the visible range of Earth's solar spectrum.

## 1.3 Objectives

The objectives of this study are as followed:

- i. To fabricate and characterize immobilized TiO<sub>2</sub>, Fe<sub>2</sub>O<sub>3</sub>/TiO<sub>2</sub> and rGO/Fe<sub>2</sub>O<sub>3</sub>/TiO<sub>2</sub> thin films to overcome the separation process.
- ii. To determine the photocatalytic activity of TiO<sub>2</sub> and Fe<sub>2</sub>O<sub>3</sub> /TiO<sub>2</sub> thin films towards the photocatalytic degradation of methylene blue (MB) dye in water.
- iii. To evaluate the effect of rGO in Fe<sub>2</sub>O<sub>3</sub>/TiO<sub>2</sub> thin film towards its photocatalytic activity in order to reduce the band gap energy.
- iv. To determine the reusability of the rGO/Fe<sub>2</sub>O<sub>3</sub>/TiO<sub>2</sub> thin film.

## 1.4 Scopes of Study

This study was focused on the fabrication, characterization, evaluation of photocatalytic activity of rGO/Fe<sub>2</sub>O<sub>3</sub>/TiO<sub>2</sub> thin film. Before fabrication of rGO/Fe<sub>2</sub>O<sub>3</sub>/TiO<sub>2</sub> thin film was done, three different materials: MIL-53(Fe), GO, and TiO<sub>2</sub> sol gel need to synthesized and prepared first. MIL-53(Fe) was synthesized using reflux method proposed by Munn and co-workers (2013). GO was

synthesized using the modified Hummers method. The obtained GO suspension was freeze dried for 24 hour to get freeze dried GO powder (Chen *et al.*, 2013; Marcano *et al.*, 2010). Meanwhile, TiO<sub>2</sub> precursor sol gel was prepared from a mixture of diethanolamine (DEA), 1-butanol, titanium (IV) butoxide (TBOT) and few drops of water (Bu *et al.*, 2005). Both TiO<sub>2</sub> sol gel and MIL-53(Fe)/TiO<sub>2</sub> sol gel were used to fabricate TiO<sub>2</sub> thin film and Fe<sub>2</sub>O<sub>3</sub>/TiO<sub>2</sub> thin film, respectively by using dip coating technique. rGO/Fe<sub>2</sub>O<sub>3</sub>/TiO<sub>2</sub> thin film was prepared by dipping the annealed Fe<sub>2</sub>O<sub>3</sub>/TiO<sub>2</sub> thin film in GO suspension followed by reduction using hydrazine vapour. Instrumentation used for characterization of synthesized materials and thin films were XRD, FTIR, UV-Vis, SEM and EDX. XRD was used to identify the crystallinity of synthesized MIL-53(Fe), GO, TiO<sub>2</sub> thin film and Fe<sub>2</sub>O<sub>3</sub>/TiO<sub>2</sub> thin film. FTIR was used to determine the functional group of synthesized GO. UV-Vis was used to analyze the synthesized GO and photocatalytic activity of thin films. The morphology and topography of TiO<sub>2</sub> thin film, Fe<sub>2</sub>O<sub>3</sub>/TiO<sub>2</sub> thin film and rGO/Fe<sub>2</sub>O<sub>3</sub>/TiO<sub>2</sub> thin film was determined using SEM. Meanwhile, EDX analysis was carried out to determine the presence of Fe<sup>3+</sup> ion and the amount of carbon in rGO/Fe<sub>2</sub>O<sub>3</sub>/TiO<sub>2</sub> thin film. Photocatalytic activity of thin films was determined using 40 mL of methylene blue (MB) solution as organic compound pollutant with initial concentration 5 ppm under UVA light irradiation for 4 hours. Reusability test was determined by using the same rGO/Fe<sub>2</sub>O<sub>3</sub>/TiO<sub>2</sub> thin film for five consecutive cycles without any activation. The photocatalytic degradation progress was determined using UV-Vis spectrophotometer.

## CHAPTER 2

### LITERATURE REVIEW

#### 2.1 Dyes and Treatment of Dye Pollutants

Dyes are colorant substance made from plants or chemicals that can be applied into a solution to a substrate and consequently giving it a coloured appearance by altering the crystal structure of the substrate (Fu., 2014). A substrate is the material where colorant is applied by using different type of processes such as dyeing, printing, surface coating and others. Some examples of substrate include of textile fibers, polymers, foodstuffs, leathers and others (Fu., 2014). Complex organic molecules of dyes usually consist of chromophore (colour bearing group) which is responsible for its colour properties. Chromophore ("*chroma*" means color and "*phore*" means bearer) basically consists of extended conjugated system in part of the dye molecules. These molecules impart its colour when it absorb visible light at certain wavelength (380 – 700 nm) and transmit the remaining light. At the same time, the presence of auxochrome ("*auxo*" means augment) in dyes molecules can greatly enhances the colour intensity.

**Table 2.1 : Names of chromophores and auxochrome group of dyes**

<b>Chromophore group</b>	<b>Name</b>	<b>Auxogroup</b>	<b>Name</b>
-N=N-	Azo	-NH <sub>2</sub>	Amino
-N=N <sup>+</sup> -O <sup>-</sup>	Azoxy	-NHCH <sub>3</sub>	Methyl amino
-N=N-NH	Azoamino	-N(CH <sub>3</sub> ) <sub>2</sub>	Dimethyl amino
-N=O, N-OH	Nitroso	-SO <sub>3</sub> H	Sulphonic Acid
>C=O	Carbonyl	-OH	Hydroxyl
>C=C<	Ethenyl	-COOH	Carboxylic acid
>C=S	Thio	-Cl	Chloro
-NO <sub>2</sub>	Nitro	-CH <sub>3</sub>	Methyl
>C=NH, >C=N-	Azomethine	-OCH <sub>3</sub>	Methoxy
		-CN	Cyano
		-COCH <sub>3</sub>	Acetyl
		-CONH <sub>2</sub>	Amido

Source: Fu *et al.*, (2014)